LEVELS OF ENDOCANNABINOIDS AND RELATED N-ACYL AMIDES CHANGE IN THE CEREBELLUM, MIDBRAIN, BRAINSTEM AND THALAMUS IN A MODEL OF ACUTE PERIPHERAL INFLAMMATION

Brandon P. Rhodes, Jordyn M. Stuart, Siham Raboune, and Heather B. Bradshaw , Indiana University, Bloomington IN

Poster #30

Background

Previous studies have demonstrated the importance of the endogenous cannabinoid system in a variety of inflammatory and pain conditions. Notably, the non-opioid component of acute stress-induced analgesia was shown to be a combination of differential signaling of 2-arachidonoyl glycerol (2-AG) and Anandamide (*N*-arachidonoyl ethanolamine; AEA) in the midbrain periaqueductal grey (Hohmann et al. 2005). In order to test the hypothesis that these findings extend to additional areas of the brain and for additional lipids, we use a model of acute peripheral inflammation that is associated with an increase in thermal and mechanical hyperalgesia and performed lipidomics screens of the midbrain, brainstem, thalamus and cerebellum for 2-AG, AEA and 79 structurally similar lipids (*N*-acyl amides and prostaglandins).

Methods

Using HPLC/MS/MS (Figure 1) we performed scans for 81 lipids (Figure 2) from methanolic extracts of MB, BS, TH, and CER in a rat model using either 3% λ-carrageenan to induce inflammation in the hindpaw or a vehicle injection (saline) as a control. Animals were sacrificed either 1 or 3 hours after injection. Lipids were partially purified from each dissected brain region on C18 solid-phase extraction columns and multiple fractions analyzed using HPLC/MS/MS optimized methods for individual lipids. Standards were purchased from Caymen Chemical or made in house. Data were compared by time point and between vehicle control (VH) and carrageenan (CG) group.

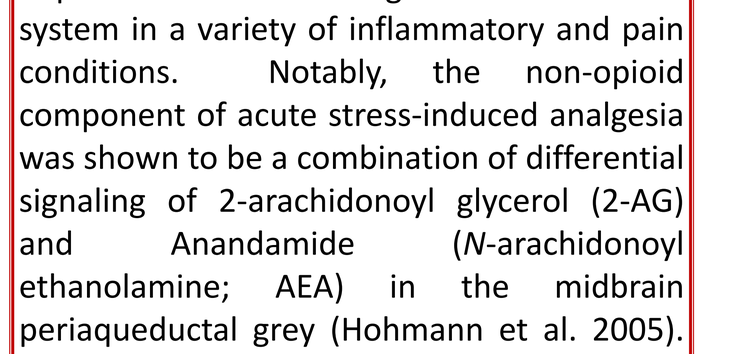

Figure 1 – Diagram illustrating HPLC/MS/MS on the API 3000 quadrupole mass spectrometer. After being partially purified on the solid phase C18 columns, analytes are further separated on reverse phase C18 analytical columns. Then, the analytes are ionized, filtered by mass, collided in vacuum, and detected.

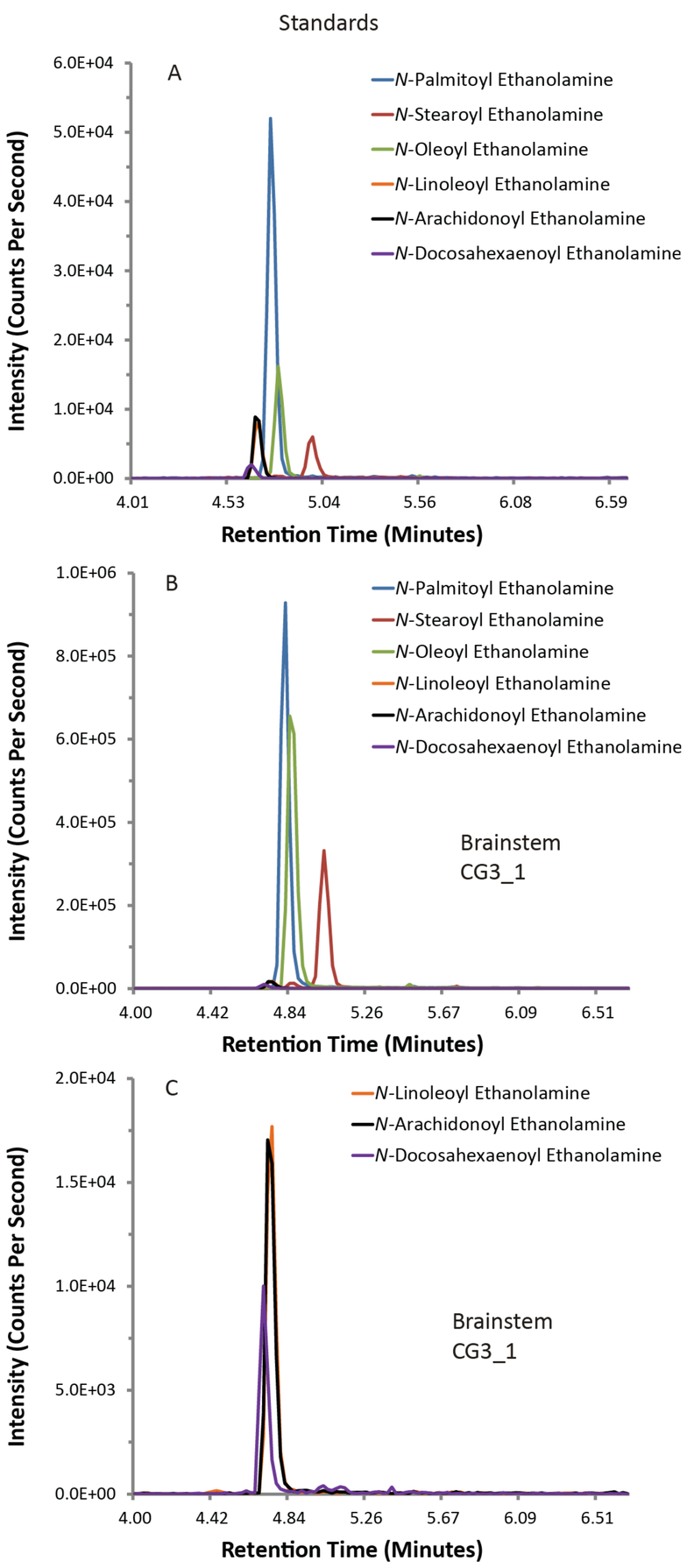

Figure 3 (Above) – Reverse phase HPLC/MS/MS output chromatograms. Data indicate that matching retention times and order of column elution verify the accuracy of the measurements in brain tissue extractions. (A) Chromatography of *N*-Acyl Ethanolamine standards. (B) Chromatography of the N-Acyl Ethanolamine methods in an elution from a brainstem extraction of a subject in the 3-hour CG treatment group. (C) A closer look at the chromatography of *N*-Linoleoyl-, *N*-Arachidonoyl-, and *N*-Docosahexaenoyl Ethanolamines.

Brainstem

N-Acyl amides	CG_1 v VH_1	CG_3 v VH_3
N-Palmitoyl ethanolamine		↑
N-Oleoyl ethanolamine		↑
N-Linoleoyl ethanolamine		↑
N-Arachidonoyl ethanolamine		↑
N-Arachidonoyl GABA	↓	

Midbrain

N-Acyl amides	CG_1 v VH_1	CG_3 v VH_3
N-Oleoyl ethanolamine		↑
N-Linoleoyl ethanolamine		↑
N-Arachidonoyl ethanolamine		↑
N-Oleoyl leucine		↑
N-Palmitoyl alanine	↓	
N-Arachidonoyl phenylalanine	↓	
Others	**CG_1 v VH_1**	**CG_3 v VH_3**
2-Arachidonoyl Glycerol	↑	

Thalamus

N-Acyl amides	CG_1 v VH_1	CG_3 v VH_3
N-Palmitoyl ethanolamine		↑
N-Oleoyl ethanolamine	↓	↑
N-Linoleoyl ethanolamine		↑
N-Arachidonoyl ethanolamine		↑
N-Docosahexaenoyl ethanolamine		↑
N-Arachidonoyl tyrosine	↑	
N-Stearoyl tryptophan	↑	

Cerebellum

N-Acyl amides	CG_1 v VH_1	CG_3 v VH_3
N-Palmitoyl ethanolamine		↑
N-Oleoyl ethanolamine		↑
N-Linoleoyl ethanolamine		↑
N-Arachidonoyl ethanolamine		↑
N-Docosahexaenoyl ethanolamine		↑
N-Stearoyl glycine		↑
N-Oleoyl glycine		↑
N-Linoleoyl serine		↑
N-Arachidonoyl glycine		↑
N-Docosahexaenoyl glycine		↑
N-Palmitoyl GABA		↑
N-Stearoyl GABA		↑
N-Oleoyl GABA		↑
N-Linoleoyl GABA		↑
N-Arachidonoyl GABA	↓	↑
N-Docosahexaenoyl GABA		↑
N-Stearoyl methonine		↑
N-Oleoyl tyrosine		↑
N-Docosahexaenoyl valine		↑
Others	**CG_1 v VH_1**	**CG_3 v VH_3**
PGE2		↑
PGF2α		↑
2-Arachidonoyl Glycerol	↑	

Figure 4: Significant changes in N-acyl amides in the carrageenan (CG) model of acute inflammation. Upwards arrows indicate a significant increase, and downward arrows indicate a significant decrease. Comparisons were made for 1-hour Veh to CG or 3-hour to CG. Analyses were oneway-ANOVA with FSL post-hoc; p<.05.

Figure 5 (Right) – Comparison of fatty-acid conjugates that changed in the carrageenan model of acute pain (data in Figure 4). All comparisons are N-acyl amide conjugates except the glycerol conjugate, 2-AG, and the arachidonic acid metabolites, PGE2 and PGF2alpha (shown in italics).

Arachidonoyl-	Oleoyl-	Stearoyl-
Ethanolamine	Ethanolamine	GABA
GABA	GABA	Glycine
Glycine	Glycine	Tryptophan
Tyrosine	Tyrosine	Methionine
Phenylalanine	Leucine	
Glycerol		
PGE2		
PGF2 a		
Palmitoyl-	**Linoleoyl-**	**Docosahexaenoyl-**
Ethanolamine	Ethanolamine	Ethanolamine
GABA	GABA	GABA
Alanine	Serine	Valine

N-Acyl ethanolamine
N-Palmitoyl ethanolamine
N- Stearoyl ethanolamine
N-Oleoyl ethanolamine
N-Linoleoyl ethanolamine
N-Arachdonoyll ethanolamine
N-Docosahexaenoyl ethanolamine
2-Arachidonoylglycerol
2-AG
***N*-Acyl glycine**
N-Palmitoyl glycine
N-Stearoyl glycine
N-Oleoyl glycine
N-Linoleoyl serine
N-Arachidonoyl glycine
N-Docosahexaenoyl glycine
***N*-Acyl serine**
N-Palmitoyl serine
N-Stearoyl serine
N-Oleoyl serine
N-Linoleoyl serine
N-Arachidonoyl serine
N-Docosahexaenoyl serine
***N*-Acyl GABA**
N-Palmitoyl GABA
N-Stearoyl GABA
N-Oleoyl GABA
N-Linoleoyl GABA
N-Arachidonoyl GABA
N-Docosahexaenoyl GABA
***N*-Acyl leucine**
N-Palmitoyl leucine
N-Stearoyl leucine
N-Oleoyl leucine
N-Linoleoyl leucine
N-Docosahexaenoyl leucine

N-Acyl methionine
N-Palmitoyl methionine
N-Stearoyl methonine
N-Oleoyl methionine
N-Linoleoyl methionine
N-Arachdonoyl methionine
N-Docosahexaenoyl methionine
***N*-Acyl tyrosine**
N-Palmitoyl tyrosine
N-Stearoyl tyrosine
N-Oleoyl tyrosine
N-Linoleoyl tyrosine
N-Arachidonoyl tyrosine
N-Docosahexaenoyl tyrosine
***N*-Acyl alanine**
N-Palmitoyl alanine
N-Stearoyl alanine
N-Oleoyl alanine
N-Linoleoyl alanine
N-Arachidonoyl alanine
N-Docosahexaenoyl alanine
***N*-Acyl threonine**
N-Palmitoyl threonine
N-Stearoyl threonine
N-Oleoyl threonine
***N*-Acyl aspartic acid**
N-Palmitoyl aspartic acid
N-Stearoyl aspartic acid
N-Oleoyl aspartic acid
N-Linoleoyl aspartic acid
***N*-Acyl valine**
N-Palmitoyl valine
N- Stearoyl valine
N-Oleoyl valine
N-Nervonoyl valine
N-Linoleoyl valine
N-Docosahexaenoyl valine

N-Acyl proline
N-Palmitoyl proline
N-Stearoyl proline
N-Oleoyl proline
N-Linoleoyl proline
N-Arachidonoyl proline
N-Docosahexaenoyl proline
***N*-Acyl tryptophan**
N-Palmitoyl tryptophan
N-Stearoyl tryptophan
N-Oleoyl tryptophan
N-Linoleoyl tryptophan
N-Arachidonoyl tryptophan
N-Docosahexaenoyl tryptophan
***N*-Acyl phenylalanine**
N-Palmitoyl phenylalanine
N-Stearoyl phenylalanine
N-Oleoyl phenylalanine
N-Linoleoyl phenyalanine
N-Arachidonoyl phenlalanine
N-Docosahexaenoyl phenylalanine
Prostaglandins
PGE2
PGF2@
N-Acyl Dopamines
N-arachidonoyl dopamine
N-oleoyl dopamine

Figure 2 – The library of the 81 lipids that were analyzed

Results and Conclusions

Several patterns were observed in lipid production among the 4 brain areas using this inflammatory model. Few changes in lipid production were measured between the VH-1hour and CG-1 hour in any of the brain areas, however, both CER and BS had a significant decrease in *N*-arachidonoyl GABA (a TRPV1 activator) and in addition, CER and MB had significant increases in 2-AG. At 3 hours post-injection, among many other changes in lipid production, all 4 brain areas had an increase in 3 *N*-acyl ethanolamines (OEA, LEA, AEA), whereas, CER and TH also showed significant increases in DHEA. No differences were measured in levels of 2-AG at 3 hours post injection in any brain area. Of the four brain areas examined here, CER had the most dynamic changes in lipid profiles with over 20 lipids changing by 3 hours post injection. Notably, while CER levels of 2-AG were significantly increased at 1 hour post injection and back to baseline at 3 hours, CER levels of the prostaglandins PGE2 and PGF2alpha were increased at 3 hours post injection, supporting recent evidence that there is a potential biosynthetic link between 2-AG and PG production (Nomura et al., 2001). These data extend and support the hypothesis that peripheral inflammation associated with pain drive changes in eCBs and related lipid mediators in the MB and other areas of the CNS.